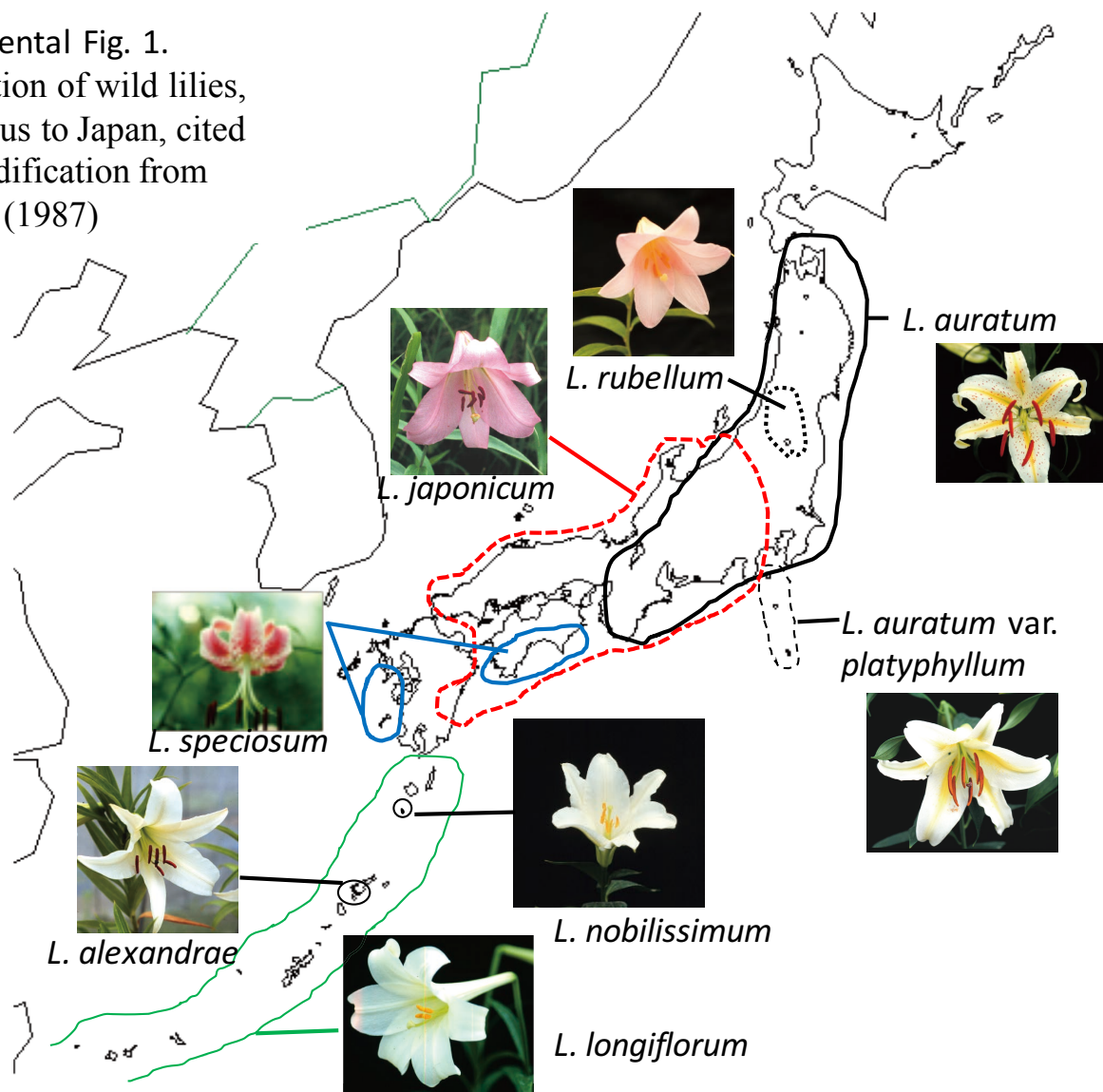
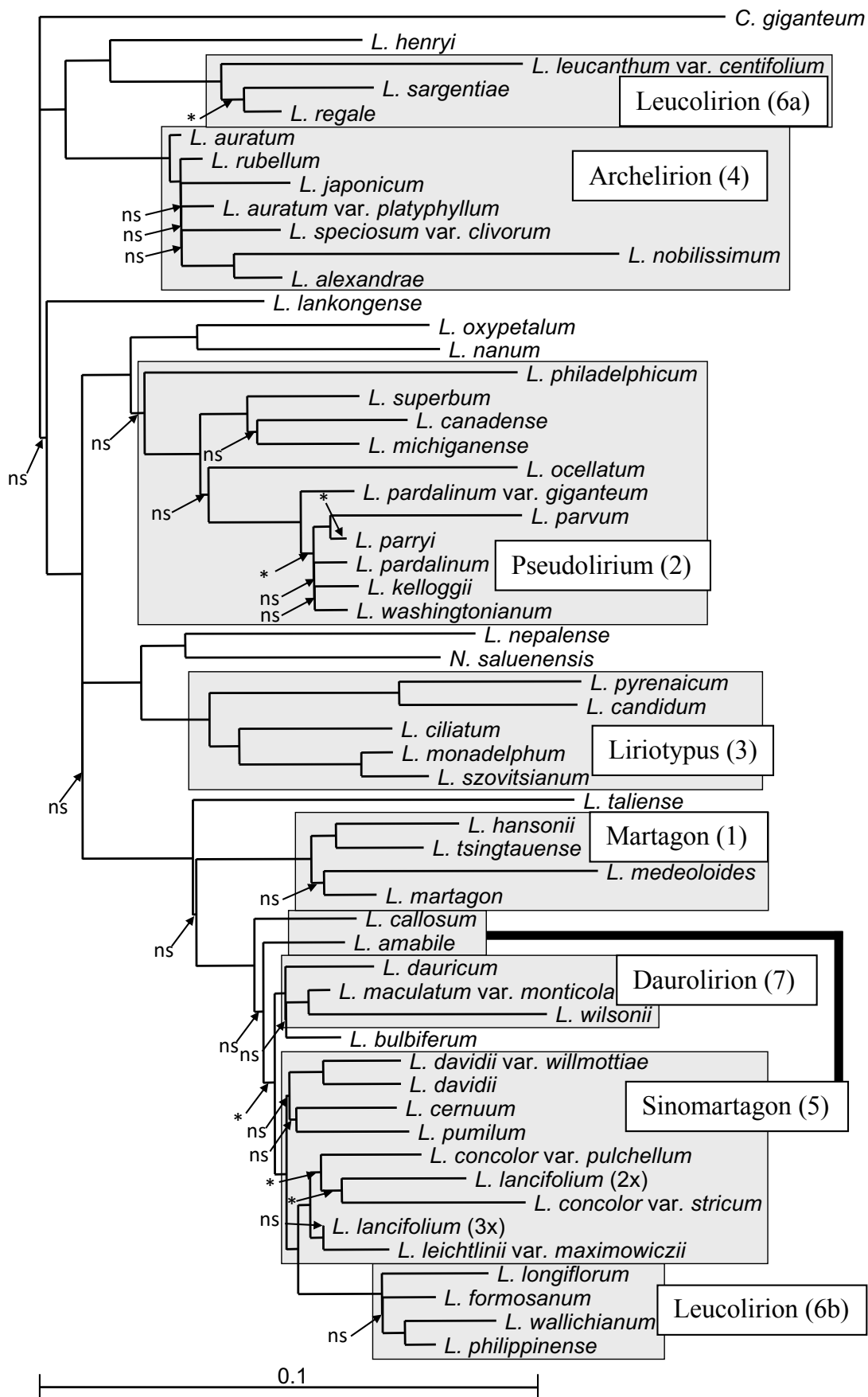
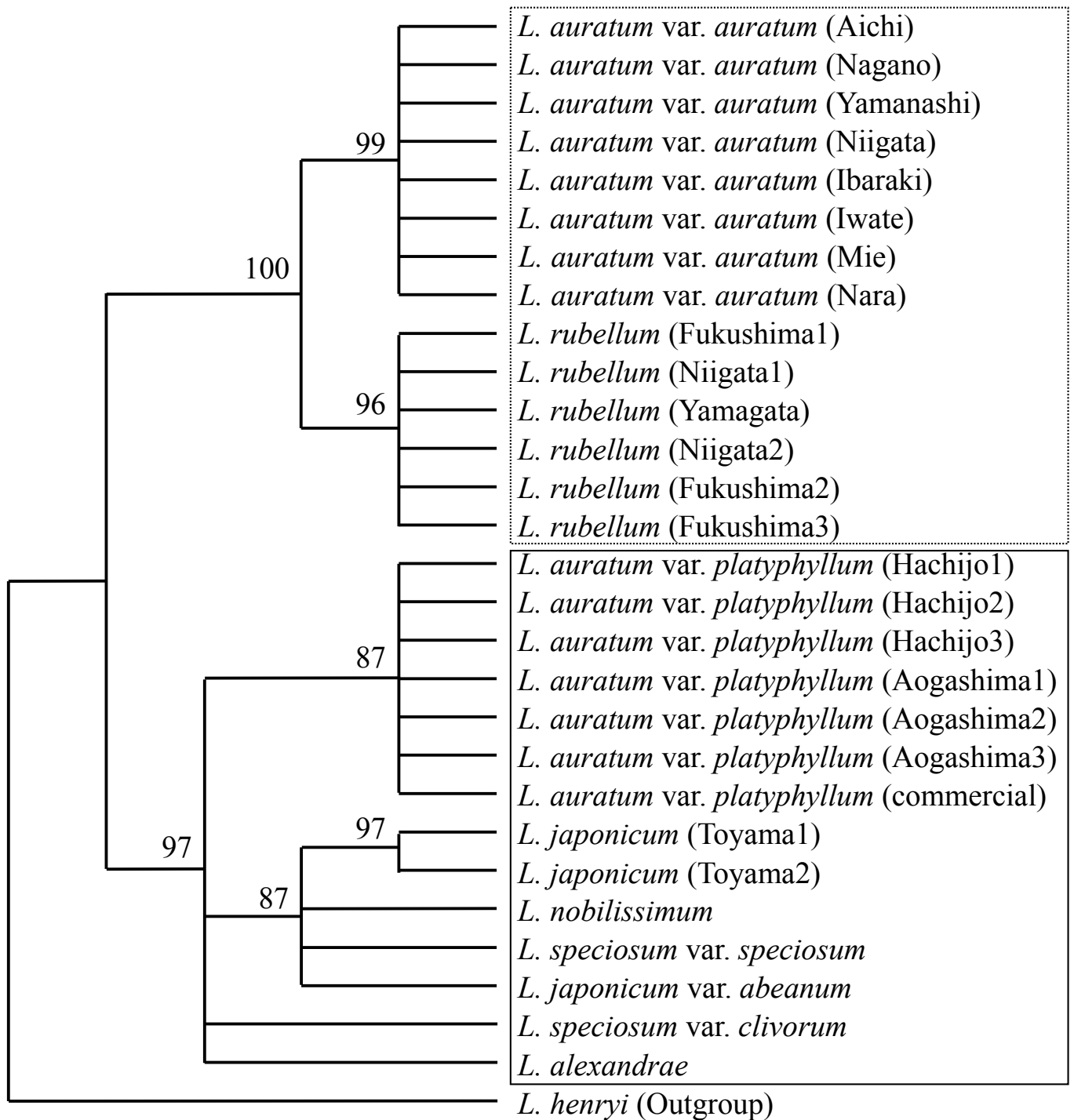


Supplemental Fig. 1.
Distribution of wild lilies,
indigenous to Japan,
cited with modification
from Shimizu (1987)

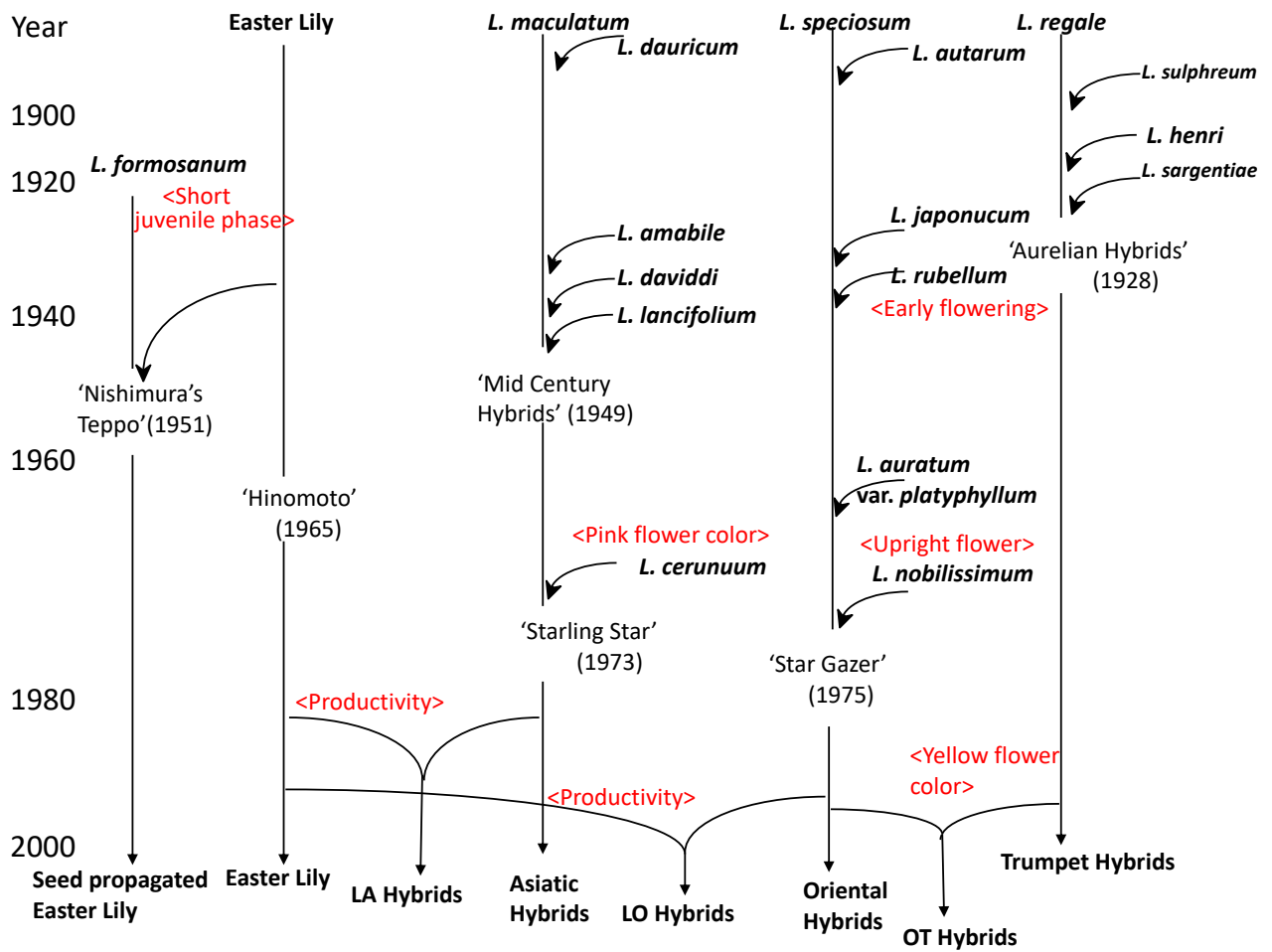




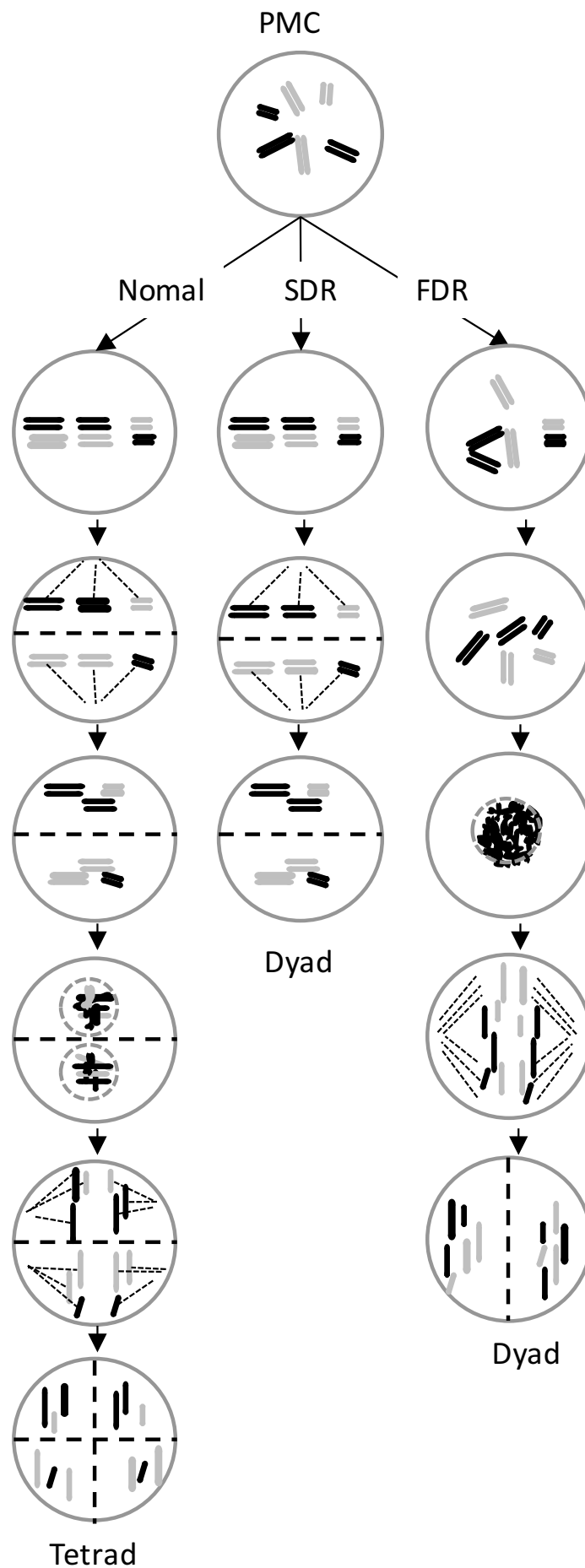
Supplemental Fig. 2. Phylogenetic tree constructed from ITS sequences of 55 *Lilium* species, *Cardiocrinum giganteum* and *Nomocharis saluenensis* by the maximum likelihood method. All branch lengths, unless otherwise indicated, are significantly positive at $P < 0.01$. Three branch lengths indicated by a single asterisk are significantly positive at $P < 0.05$. Twenty branch lengths indicated by "ns" are not significantly positive. Section clusters are shaded and labeled with the section name and number; *L. bulbiferum* are excluded from the Liriotypus shaded box, and six species (*L. henryi*, *L. lankongense* and subsection 5c species) also excluded from the Sinomartagon shaded box, because their locations are out of the classified cluster.



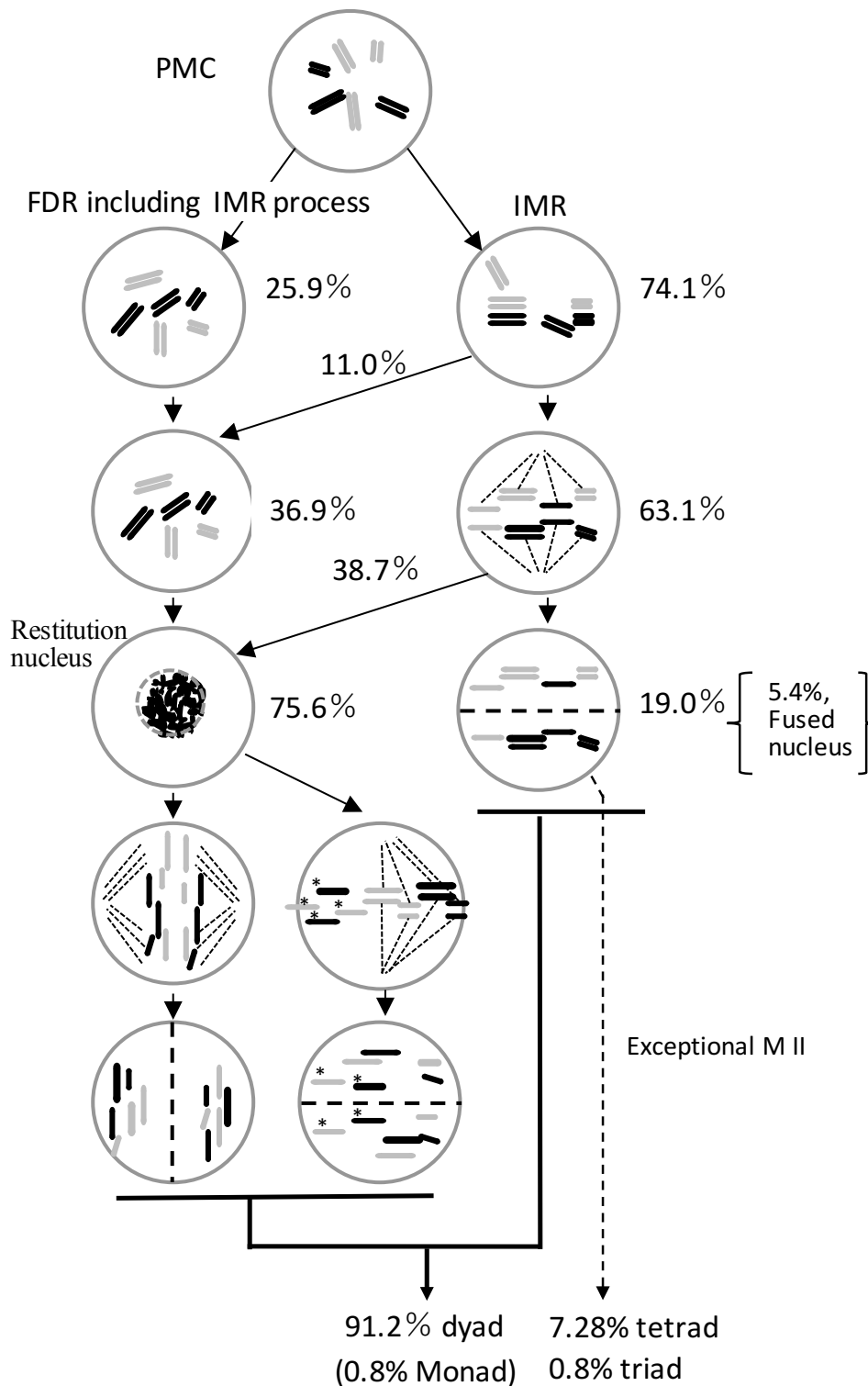
Supplemental Fig. 3. Phylogenetic tree of section Archelirion of genus *Lilium* based on sequence data of three chloroplast DNA regions using the maximum parsimony method. The tree is strict consensus of the eight most parsimonious trees. Tree length = 58, Consistency index (CI) = 0.8966, Retention index (RI) = 0.9791, Rescaled consistency index (RC) = 0.8778. The numbers above the nodes represent bootstrap value expressed as percentage of 1,000 bootstrap replications. Each box shows similarity of cytoplasm.



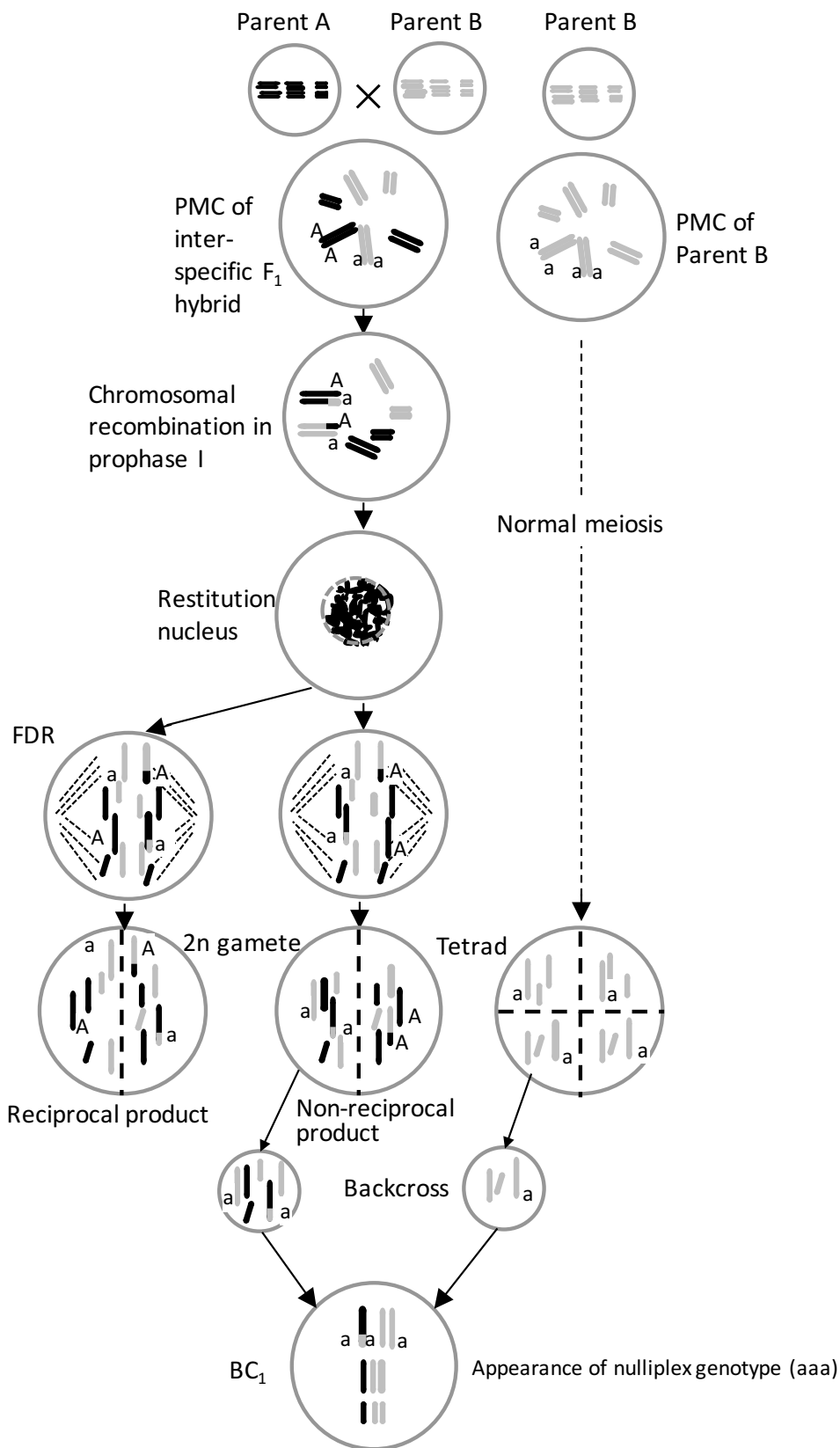
Supplemental Fig. 4. History of lily breeding. The diagram is depicted based on the references written by Jefferson-Brown (1988), Leslie (1982), and Shimizu (1987). The agronomic traits transmitted from wild species or cultivars are indicated by the brackets.



Supplemental Fig. 5. Schematic diagram of meiotic restitution for producing $2n$ gametes in a hybrid. For clarity only three pairs of homoeologous chromosomes of the respective species (back and gray) and an example of the chromosome assortment are shown. PMC; pollen mother cell, FDR; first division restitution, SDR; second division restitution, IMR; indeterminate meiotic restitution, Dyad; two microspores, Tetrad; four microspores.



Supplemental Fig. 6. Schematic diagram of meiotic restitution for producing 2n gametes in the hybrid, *L. auratum* × *L. henryi* (AuH) cited with modification from Asano (1984). * indicates that at the diakinesis stage univalents are randomly separated into each gamete. PMC; pollen mother cell, FDR; first division restitution, IMR; indeterminate meiotic restitution, MII; second meiotic division, Dyad; two microspores, Tetrad; four microspores.



Supplemental Fig. 7. Schematic diagram of formation of a nulliplex allele (aaa) generated in a BC₁ plant by fusing of n gamete from the recurrent parent and 2n FDR gamete having chromosomal recombination in the interspecific hybrid. PMC; pollen mother cell, FDR; first division restitution, Tetrad; four microspores.

subgenus *Clusianae*

T. chysantha

T. maximowczii



subgenus *Eriostemones*

T. urumiensis



T. sylvestris

T. hageri

T. saxatilis



subgenus *Tulipa*

T. kolpakowskiana

T. praecox

T. eichleri 'Maxima'



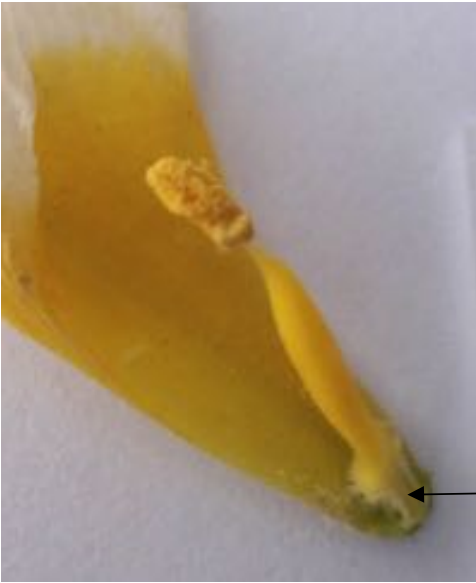
T. schrenkii

T. kaufmanniana

T. fosteriana

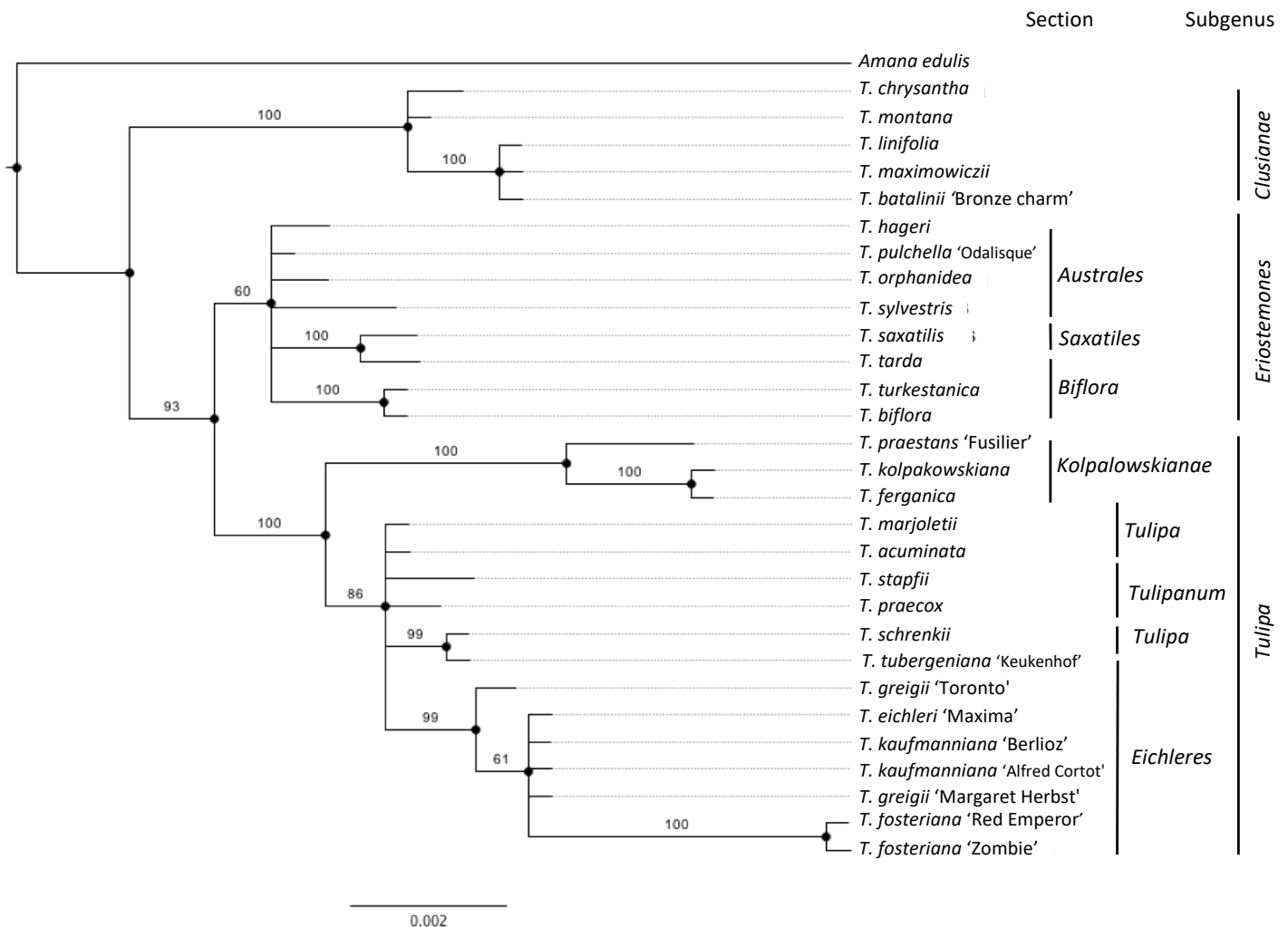


Supplemental Fig. 8. Some species classified into the three subgenera of the genus *Tulipa*.



Supplemental Fig. 9. Hairy boss at base of filaments that is a key character for distinguishing the species belonging to subgenus *Eriostemones*.

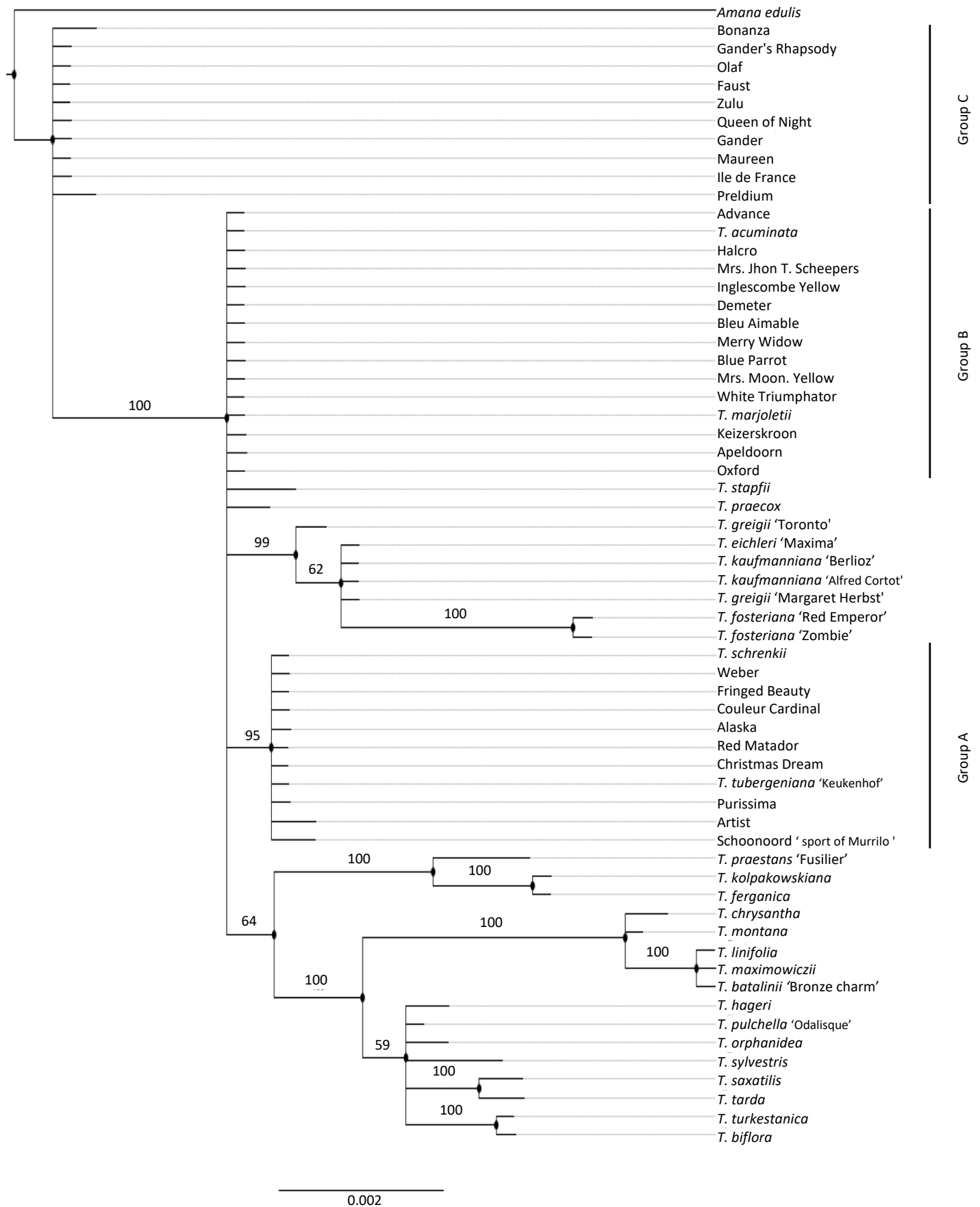
Erio- = wool



Supplemental Fig. 10. Phylogeny of 29 species of *Tulipa* and *Amana edulis*

T. chrysantha

The genomic sequences of *Maturase K* (*matK*) and *trnT-L* for *Amana edulis* and twenty-nine species of the genus *Tulipa* were concatenated into a supergene and aligned by clustalw. The multiple sequence alignment (MSA) was then filtered for poorly aligned positions and divergent regions using gblocks. The conserved blocks were then used for phylogenetic analysis by Bayesian inference using Mr. Bayes (version 3.2). The Monte-Carlo Markov Chain (MCMC) used 1,000,000 generations with a burn-in of 250,000 generations and 5 chains. Nodes display their posterior probabilities as a percent of sampled trees containing them, taken from the total pool of 1,000,000 generations and sampled every 1,000 generations (1,000 trees). The scale bar indicates expected substitutions per site. The DNA sequences of *matK* and *trnT-L* can be accessed with the following GenBank accessions BankIt2049259 (MG026731 - MG026771) and BankIt2052094 (MG026772 - MG026836).



Supplemental Fig. 11. Phylogeny of 29 species and 33 cultivars of *Tulipa* and *Amana edulis*

The genomic sequences of *Maturase K* (*matK*) and *trnT-L* for *Amana edulis* and sixty-two species of the genus *Tulipa* were concatenated into a supergene and aligned by clustalw. The multiple sequence alignment (MSA) was then filtered for poorly aligned positions and divergent regions using gblocks. The conserved blocks were then used for phylogenetic analysis by Bayesian inference using Mr. Bayes (version 3.2). The Monte-Carlo Markov Chain (MCMC) used 1,000,000 generations with a burn-in of 250,000 generations and 5 chains. Nodes display their posterior probabilities as a percent of sampled trees containing them, taken from the total pool of 1,000,000 generations and sampled every 1,000 generations (1,000 trees). The scale bar indicates expected substitutions per site. The DNA sequences of *matK* and *trnT-L* can be accessed with the following GenBank accessions BankIt2049259 (MG026731 - MG026771) and BankIt2052094 (MG026772 - MG026836).